ENVIRONMENTAL STUDIES

Solar irradiance and ENSO affect food security in Lake Tanganyika, a major African inland fishery

M. M. McGlue[1]*, S. J. Ivory[2], J. R. Stone[3], A. S. Cohen[4], T. M. Kamulali[4], J. C. Latimer[3], M. A. Brannon[1†], I. A. Kimirei[5], M. J. Soreghan[6]

Food security in a warming world is a grave concern for rapidly growing impoverished populations. Low-latitude inland fisheries provide protein for millions of rural poor, yet the impacts of high-frequency climate oscillations on these aquatic ecosystems are unknown. Here, we present a sub-annual–to–annual resolution paleolimnological reconstruction of upwelling, productivity, and algal composition at Lake Tanganyika, one of Africa's largest land-locked fisheries. The data reveal increases in diatom production at centennial-scale solar irradiance maxima, and interannual variability in upwelling linked to La Niña. Our study shows that interactions between global climatic controls and El Niño–Southern Oscillation teleconnections exert profound influences on the foundation of Lake Tanganyika's food web. Adapting long-term management practices to account for high-frequency changes in algal production will help safeguard inland fish resources.

INTRODUCTION

Inland fisheries play disproportionately large roles in the food and economic security of many developing nations, and the health and cultural identity of vast numbers of rural poor are interwoven with fishing (*1*–*2*). In Africa, the consequences of climate change for inland fisheries are not well understood. The Intergovernmental Panel on Climate Change reports that marine fisheries in the tropics are at high risk due to warming, but extensive data on the response of inland fisheries are unavailable (*3*). Reduced availability of larger species, coupled with high demand, has placed new emphasis on managing fisheries rich in small pelagic fish, including Lake Tanganyika, one of Africa's oldest and largest lakes (Fig. 1A). Small pelagic fish such as herring (Clupeidae) now represent almost three quarters of the total inland fish catch within Africa (*4*). These smaller, open-water species are highly productive, easy to catch, and amenable to preservation (*5*). At Lake Tanganyika, the endemic clupeids (known locally as *dagaa*) play a crucial role in both trade and nutrition for coastal populations. *Dagaa* are secondary consumers in Lake Tanganyika's simple pelagic food web, which is strongly reliant on bottom-up controls (*6*). This means that greater algal production results in more *dagaa* and other economically valuable fish, like the endemic perch *Lates stappersii*. Knowledge of how the pelagic food web responds to external forcing factors like climate is critical for identifying vulnerabilities and maintaining healthy stocks (*7*).

Historical records of air temperature, conductivity, and wind speed have shown that a warmer Lake Tanganyika correlates with lower primary production and fish catch (*8*–*9*). These studies suggest that the resilience of Lake Tanganyika's pelagic food web declines with warming, which strengthens water column stratification and reduces nutrient availability by curtailing upwelling. Recent low-resolution sediment core studies have demonstrated that lake surface temperatures have varied perhaps as much as ~1° to 3°C during the past several millennia, and argue that simple radiative forcing controls primary production (*10*–*11*). Yet much is still unknown about climatic influences on Lake Tanganyika's pelagic food web, and existing low-resolution paleolimnological data are impossible to link to mechanisms driving ecosystem variability at time scales relevant for informing fisheries management. Effective stewardship of Lake Tanganyika's fisheries requires that observations from sedimentary paleo-records form a direct bridge to conservation strategies, which means that the time scales of both must be compatible. Detailed information on upwelling, nutrient dynamics, food web interactions, and their relationships to climatic modes that vary on interannual scales, such as the El Niño–Southern Oscillation (ENSO), are critically important but unfortunately unavailable. Thus, to understand the influence of high-frequency atmospheric changes on upwelling and algal ecological dynamics at Lake Tanganyika, data from well-preserved and accurately dated sediment cores with high temporal resolution are needed.

Tracking upwelling at Lake Tanganyika

Lake Tanganyika is meromictic (permanently stratified and anoxic below ~100 to 150 m) (*10*), but stratification weakens seasonally from upwelling, the process by which deep, eutrophic waters rise and fertilize surface waters, increasing photosynthesis and phytoplankton biomass. Upwelling occurs in the austral winter dry season (May to September), when the tropical rain belt is in the northern hemisphere and Lake Tanganyika is under the influence of the Indian Ocean monsoon. Dry southeast monsoon winds blowing up Lake Tanganyika's long axis push surface waters northward and set up a deep, southerly directed return current that causes upwelling in the lake's southern basin (*12*). Dry season upwelling results in a high mixing depth–to–euphotic zone depth ratio, deep (up to 300 m) incursions of O_2 and low light levels in the water column, and extensive diatom blooms as nutrient availability increases (*12*–*13*). Diatoms are single-celled, photosynthetic siliceous algae that form the foundation of Lake Tanganyika's pelagic food web, with transfer of energy to *dagaa* either directly when the fish are juveniles or following grazing by calanoid copepod zooplankton (*14*). In particular, diatoms belonging to the genus *Nitzschia* thrive when convective

[1]Department of Earth and Environmental Sciences, University of Kentucky, Lexington, KY, USA. [2]Department of Geosciences and Earth and Environmental Systems Institute, Pennsylvania State University, University Park, PA, USA. [3]Department of Earth and Environmental Systems, Indiana State University, Terre Haute, IN, USA. [4]Department of Geosciences, University of Arizona, Tucson, AZ, USA. [5]Tanzania Fisheries Research Institute, Dar es Salaam, Tanzania. [6]School of Geosciences, University of Oklahoma, Norman, OK, USA.
*Corresponding author. Email: michael.mcglue@uky.edu
†Present address: Department of Earth Sciences, Syracuse University, Syracuse, NY, USA.

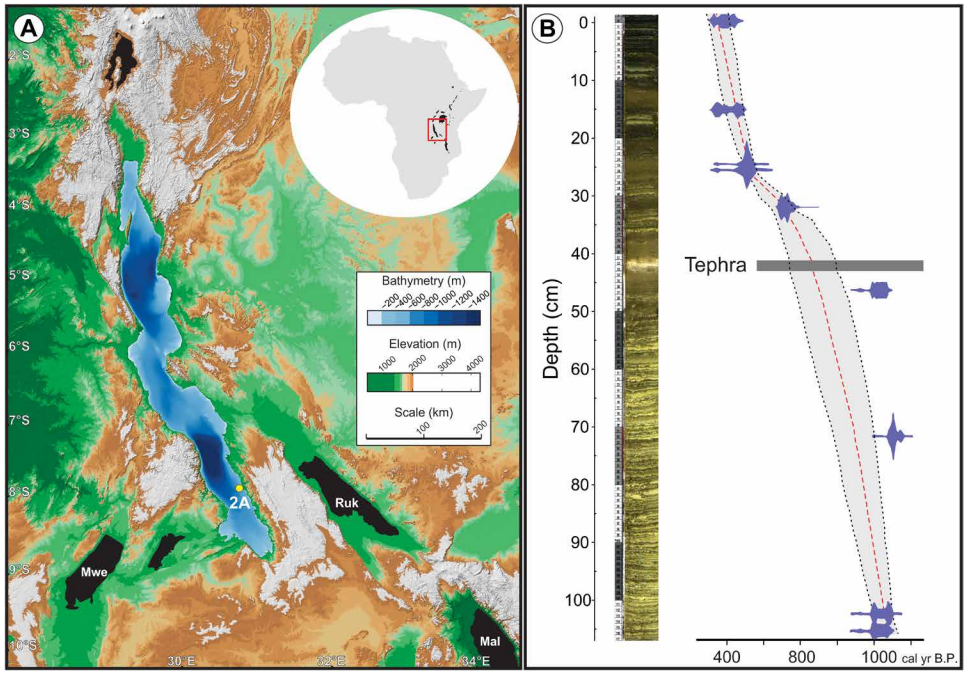

Fig. 1. Lake Tanganyika. Inset map (A, upper right) shows the position of the lake in the east African rift valley. (**A**) Digital elevation and bathymetric data (courtesy tcarta.com) illustrate the topography and hydrography of the lake and its watershed. Other large lakes appear in black, and several support important regional fisheries. Mal, Lake Malawi; Ruk, Lake Rukwa; Mwe, Lake Mweru. Core LT17-2A (yellow dot) was collected from an outer ramp depositional setting (~420-m water depth) in Lake Tanganyika's southern basin. (**B**) High-resolution core photo and Bacon-derived radiocarbon age-depth model. The core consists of laminated diatom ooze, structureless clayey silts, tephra, and sapropel and spans the interval ~670–1610 CE. The blue markers, dotted red line, and gray shading represent calibrated radiocarbon control points, the best age model solution based on the mean age for each depth, and 95% confidence interval, respectively.

mixing advects phosphorus (P), silicon (Si), and nitrogen (N) from depth (*15*). Planktic *Nitzschia* are strong competitors when N is a limiting nutrient and are often associated with cyanobacteria that are critical to the food web because they fix nitrogen in the water column. *Nitzschia* species produce lightly silicified cell walls (frustules), and the lake's Si-poor waters often result in substantial valve dissolution before burial. In deepwater sediments, preservation of *Nitzschia* requires periods of vigorous productivity, which enhances sinking and burial rates. During periods of lower diatom productivity and limited nutrients, only centric diatoms with more robust valves such as *Aulacoseira* and *Cyclostephanos* are preserved in sediments.

Dry season winds result in a longitudinally tilted epilimnion (surface layer) and thermocline (*13*). At the transition to the rainy season (October to April), the winds weaken and change direction as the tropical rain belt migrates southward. Lake Tanganyika begins to restratify, and its surface layer oscillates; the strength of the oscillation is proportional to dry season wind speeds (*12*). This process forms or reactivates seiches (internal waves) around the thermocline that results in patchy secondary upwelling along the ends of the lake, which releases biologically available nitrates, P, and iron to the surface layer (*16*). Cyanobacteria, including the N_2-fixing picoplankton *Synechococcus*, flourish under these reduced nutrient, high light conditions as the water column stabilizes (*17*–*18*). Cyanobacteria are more competitive for low-moderate P as the lake restratifies, in part because diatom blooms from dry season upwelling exhaust bioavailable Si in the epilimnion. This Si, trapped in the frustules of settling diatoms during the rainy season, is ultimately buried in lake floor sediments or remineralized before the next dry season. On the other hand, P cycling is analogous to a battery in Lake Tanganyika (*19*), and its availability to phytoplankton is influenced by climate and landscape processes (multi-centennial time scale external nutrient loading) and upwelling (annual-to-decadal time scale internal nutrient loading). Recharge of P requires chemical weathering and runoff to deliver phosphate to the lake, where it is sequestered at depth. Upwelling transports dissolved P to the photic zone, where algae exploit it.

Here, we present new geochemical (Si/Ti, Fe/Mn, Ti, $\delta^{15}N$, and total P) and paleoecological (diatom) data from laminated sediment core LT17-2A, collected near the locus of upwelling in southern Lake Tanganyika (Fig. 1B). The core was dated using radiocarbon (^{14}C), and our age-depth model shows that the record spans ~670–1610 CE after accounting for corer disturbance and Lake Tanganyika's old carbon reservoir (Supplementary Materials). Reservoir-corrected ^{14}C ages were used to develop an age-depth model using Bacon for R (*20*). The resulting age model has a long-term sedimentation rate of 0.12 cm/year, which is consistent with accumulation rates derived from other studies (*21*). The analysis revealed considerable variability in upwelling, algal composition, and nutrient dynamics over the period of record.

RESULTS

Si/Ti chemostratigraphy exhibits a long-term trend of high values from ~670 to 1000 CE, with evidence of interannual variability (Fig. 2A). High Si/Ti corresponds sedimentologically to laminated diatom ooze and indicates high productivity driven by vigorous dry season upwelling (fig. S1). A transition occurs at ~1000–1100 CE, where Si/Ti declines and only small peaks are present (Fig. 2A).

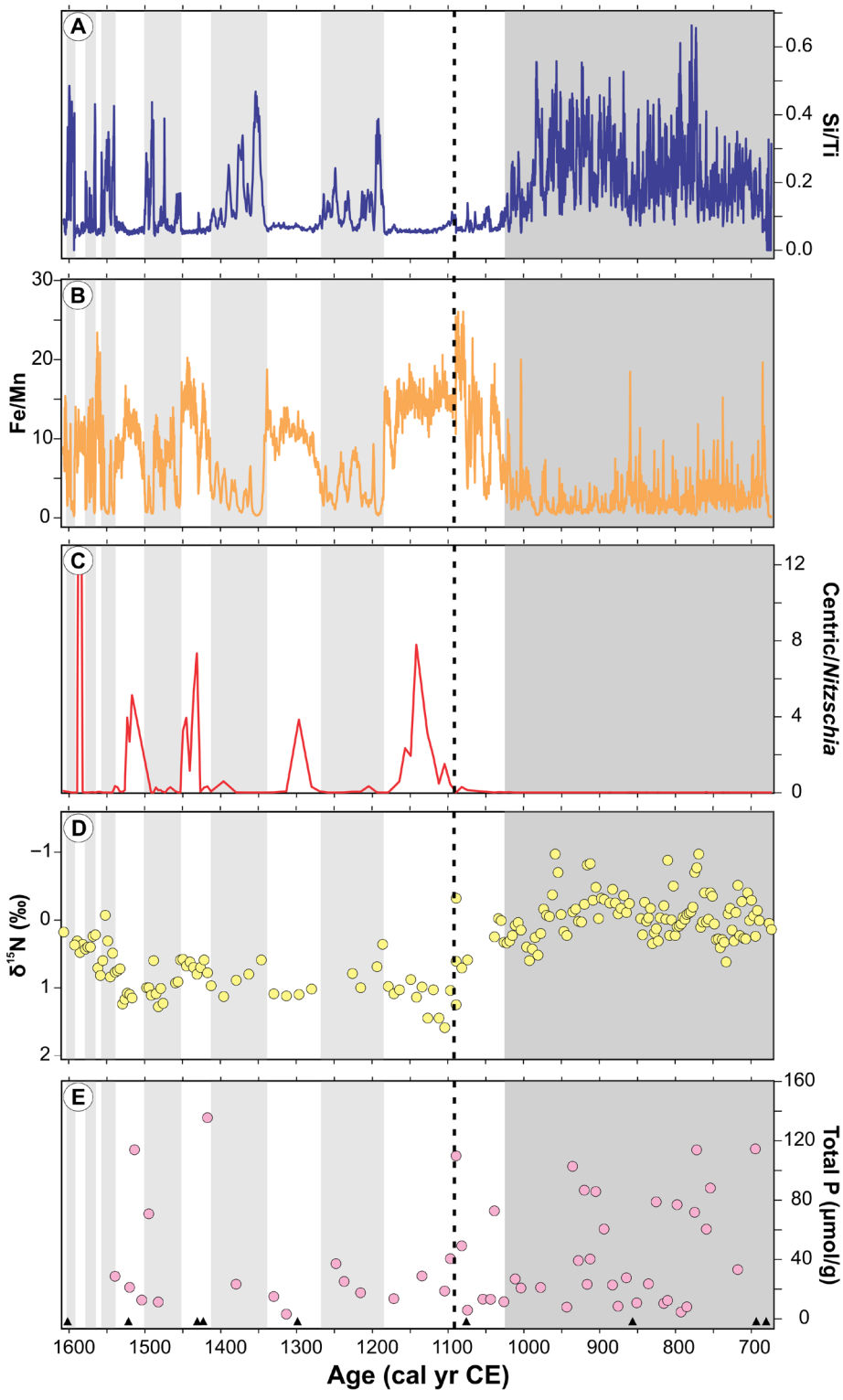

Fig. 2. Multiple geochemical and paleoecological indicators used to reconstruct upwelling, primary production, and algal composition in southern Lake Tanganyika, ~670–1610 CE. Gray shading indicates periods of inferred upwelling. Stippled bar indicates location of tephra bed. Black triangles indicate radiocarbon control points. The scale on the $\delta^{15}N$ is inverted; all other values increase upward. (**A**) Si/Ti chemostratigraphy. High values indicate elevated diatom production induced by upwelling. (**B**) Fe/Mn chemostratigraphy. Low values indicate lake ventilation associated with water column mixing and upwelling. (**C**) Centric/*Nitzschia* diatoms. *Nitzschia* requires dissolved silica in the photic zone, derived from upwelling, to be productive enough to dominate the fossil assemblage. (**D**) $\delta^{15}N$ chemostratigraphy. Units are in ‰. Prevalence of diazotrophic cyanobacteria associated with upwelling results in lower values. (**E**) Total phosphorous (P) chemostratigraphy. Units are in μmol/g. High total P accompanies upwelling and elevated primary productivity, resulting in less nutrient recycling (see text for details).

This indicates a change in upwelling, although dilution from a tephra layer influences part of this interval (Supplementary Materials). The Si/Ti curve changes markedly after ~1100 CE, with episodic peaks at ~1180–1270 CE, ~1340–1410 CE, ~1450–1500 CE, and ~1540–1600 CE associated with thin bundles of laminated ooze (Fig. 2A). These sediments are intercalated with structureless brown-black muds characterized by moderate to high Fe/Mn (Fig. 2B). The high Fe/Mn data indicate stable water column stratification, because the solubility of both elements increases in a reducing environment, but Mn is more sensitive (*22*–*23*). Fe/Mn and Si/Ti are antiphased virtually throughout the record, suggesting a common controlling mechanism. Upwelling is the best explanation, because a strongly stratified water column limits nutrient recharge to the photic zone and constrains diatom production. These interpretations are corroborated by the ratio of centric-to-*Nitzschia* diatoms, which responds to high planktic diatom productivity and reflects the burial rate and preservation dynamics of silica frustules (*24*). *Nitzschia* dominates the plankton communities when Si/Ti is high, whereas intervals of low Si/Ti generally favor the more robust centric diatoms (Fig. 2C). Higher relative abundances of centric diatoms, but substantially lower total abundances, occur when high Fe/Mn indicates a strongly stratified water column. In those periods, Si was limited and diatom dissolution was very likely commonplace (Fig. 2C).

The occurrence of cyanobacteria associated with upwelling and seiche activity was inferred using $\delta^{15}N$, because little fractionation occurs during N_2 fixation, resulting in $\delta^{15}N \leq 0‰$. In contrast, N cycling (e.g., remineralization to dissolved species) in the water column before assimilation by diatoms results in more positive isotopic values (*25*). The $\delta^{15}N$ data exhibit coherent trends with Si/Ti, Fe/Mn, and centric/*Nitzschia* (Fig. 2D). From ~670 to 1000 CE, $\delta^{15}N$ is rather low, averaging −0.07‰ with minima below −0.8‰, consistent with the presence of N_2-fixing cyanobacteria and strong seiches as the seasonal winds shifted. Our data suggest a similar set of processes toward the end of the record, around 1540 to 1600 CE, with high Si/Ti, abundant *Nitzschia*, and low $\delta^{15}N$. Both intervals occurred when Lake Tanganyika experienced relatively cool surface waters, based on the previously published temperature reconstruction of Tierney *et al.* (*11*) (Fig. 3). $\delta^{15}N$ generally is more positive from ~1000 to 1100 CE (mean = ~0.35‰), and values diagnostic of N_2 fixation are uncommon (Fig. 2D). This change is consistent with the transition to lower Si/Ti over the same period. From ~1100 to 1610 CE, $\delta^{15}N$ is relatively high (>1‰) during periods when Si/Ti and Fe/Mn indicate stable water column stratification, whereas $\delta^{15}N$ declines when pulses of upwelling occur, contrary to a simple model that would predict high N_2 fixation during stratified intervals. $\delta^{15}N$ values never drop below ~0‰ from ~1100 to 1400 CE, a period marked by warm surface waters (Fig. 3) (*11*). These data show that although short-lived (multi-decadal) pulses of upwelling were occurring during instances of lake warming, the seasonal phytoplankton succession faltered ~1100–1400 CE.

Additional insights into nutrient status within the upwelling system were gained through P geochemistry, which includes oxide, organic, and mineral components. From ~670 to 1000 CE, total P burial reaches maximum values (Fig. 2E), with an average of 47.2 μmol/g. The mineral phase dominates, whereas the organic and oxide phases are lower (fig. S2). Strong upwelling and primary productivity are implied by these data, as less recycling is occurring, corroborating Si/Ti and centric/*Nitzschia* trends from the same interval. Elevated total P values likewise indicate that rainfall was adequate to recharge the deep P pool from ~670 to 1000 CE (Fig. 2E). Total P declines ~1100 CE, and thereafter, high values are rare. These data indicate lower productivity ~1100–1400 CE, but it is possible that P was limited in the water column, as is implied by more positive values of $\delta^{15}N$. A weak dry season monsoon would explain this pattern; low wind speeds were insufficient to promote seiches, and/or reduced rainfall depleted the deep P reservoir. High values of total P occur at ~1420, 1500, and 1510 CE (Fig. 2E). In these cases, both organic and mineral P were elevated (fig. S2), signaling transient wet intervals resulting in greater allochthonous P transport to Lake Tanganyika. Titanium chemostratigraphy data indicate higher erosion to the lake ~1410–1460 CE and 1500–1540 CE, which helps to explain elevated P during those periods (fig. S3).

Atmospheric controls on the upwelling system

Wavelet analysis of the Si/Ti data shows significant power at 256- and 512-year frequencies over the full record and significant power at 2- to 12-year frequencies across certain intervals (Fig. 4). Solar irradiance oscillates over several multi-centennial frequencies and has been implicated as an important mechanism of global environmental change, including the hydroclimate of the past 100 years at Lake Victoria, another critical landlocked fishery in sub-Saharan Africa (*26*–*28*). Solar irradiance is the amount of energy from the Sun that reaches the top of Earth's atmosphere, and the tempo of the de Vries (~200 years) and North Atlantic (~550 years) solar cycles are similar to the frequencies identified by the wavelet analysis. Because upwelling is linked to the monsoon, the best explanation for the relationship between global climate and algal production in southern Lake Tanganyika is cyclic strengthening of the monsoon with changes in solar intensity. Meteorological data help corroborate that interpretation, as the boreal summer (June to August) monsoon is amplified because of intensification of Hadley and Walker circulation during solar irradiance maxima (*29*). Modeling experiments further suggest stronger trade winds associated with solar forcing of tropical convection and precipitation (*30*).

Solar irradiance in the Common Era (*31*) shows a correspondence between maxima and most Si/Ti peaks in LT-2A, the limitations inherent to ^{14}C dating notwithstanding (Fig. 3). Yet solar irradiance increased from ~1060 to 1245 CE and reached a maximum by ~1140 CE, without a correspondingly broad, centuries-long peak in Si/Ti. The start of this interval falls within the ~1000–1100 CE transition zone, when Si/Ti values declined and Fe/Mn increased (Fig. 2). *Nitzschia* dominated ~1000–1100 CE, indicating vigorous diatom production and preservation, while total P and $\delta^{15}N$ varied, with a few values indicative of transient vertical nutrient flux. These geochemical and paleoecological signals are consistent with the inception of changes to the upwelling system, most likely attributable to increasingly stable water column stratification and a weakening monsoon. Proxy reconstructions of temperature (*11*) show that lake warming occurred from ~1040 to 1400 CE and overlapped the Medieval Climate Anomaly (MCA) (Fig. 3) (*32*). Lake surface temperature therefore appears to serve as a tipping point, with warming triggering a faltering in upwelling. Vigorous dry season upwelling apparently resumed near the peak of solar irradiance in the Medieval Maximum, as Si/Ti and *Nitzschia* increased and Fe/Mn decreased at ~1180 CE (Fig. 2). However, the anticipated peaks in P and $\delta^{15}N$ are absent, suggesting an environmental change that affected phytoplankton succession. Low rainfall and weak winds would explain the pattern we observe in the data, by limiting recharge of the deep P reservoir and minimizing

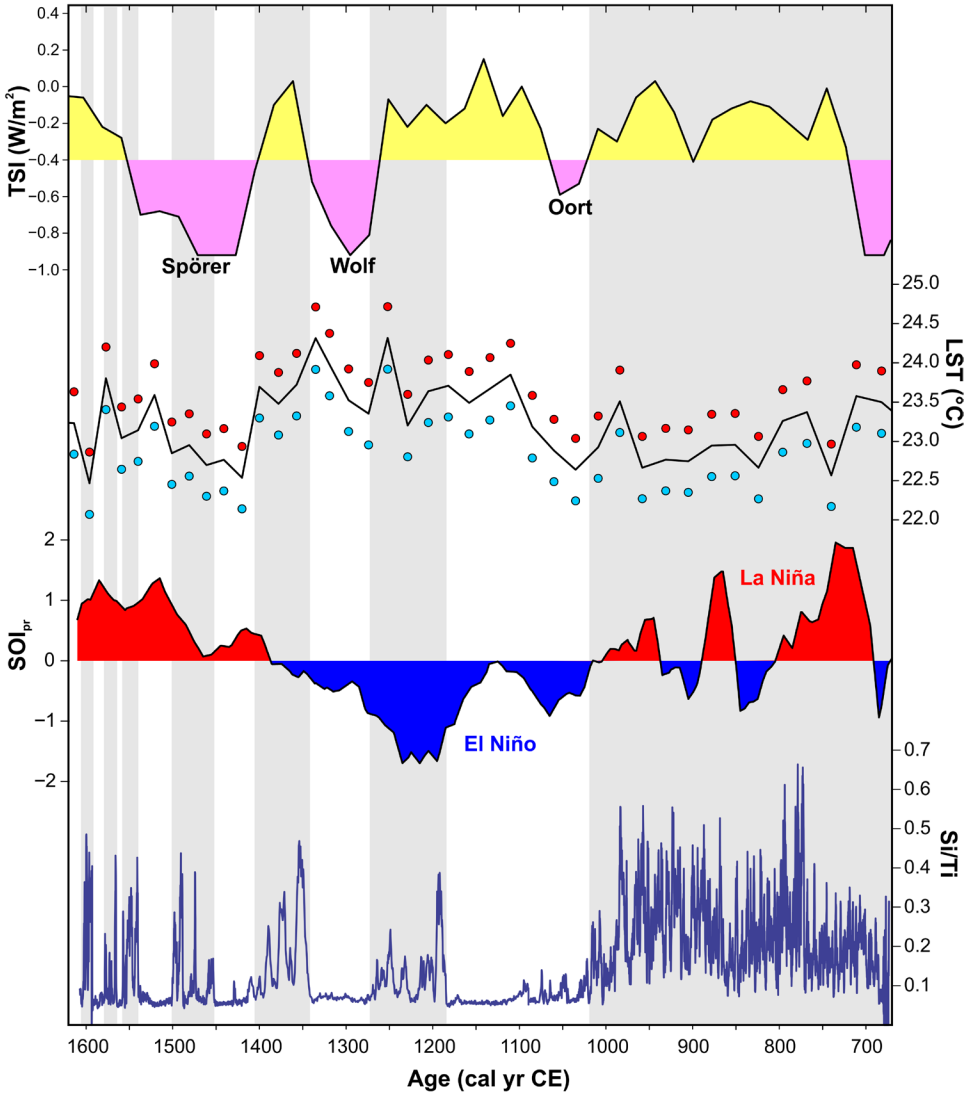

Fig. 3. Proxy data comparison. Comparison of paleoclimate proxy data [change in total solar irradiance (TSI) (*31*), Lake Tanganyika surface warming (*11*), and Southern Oscillation Index (SOI) precipitation reconstruction (*37*)] with Si/Ti chemostratigraphy from core LT17-2A. Red and blue dots represent high and low estimates surrounding the mean (solid line) of the lake temperature record, respectively. Strong evidence of upwelling and diatom production in southern Lake Tanganyika is associated with solar irradiance maxima, La Niña–like conditions, and cool lake surface water, whereas solar irradiance minima, El Niño, and warm surface waters limit upwelling and algal production. LST, Lake surface temperature.

seiches, upon which cyanobacteria are dependent. Evidence from northern Lake Tanganyika suggests that the MCA was dry (*33*). Titanium chemostratigraphy (fig. S3) confirms that detrital flux to the lake declined ~1180–1400 CE, consistent with lower rainfall and a weaker monsoon at this time. Weakening of the monsoon over southern Lake Tanganyika ~1180–1400 CE has linkages to ENSO forcing and is consistent with more El Niño–like conditions in the tropical Pacific Ocean (Fig. 3).

The chief mode of global climate variability at interannual time scales (~2–7 years) is ENSO, but until our study, sedimentary records from Lake Tanganyika lacked the resolution needed to unequivocally detect this forcing. Nevertheless, meteorological studies of Africa have emphasized ENSO controls on the monsoon (*34*–*35*). Each package of laminated diatom ooze (~670–1000 CE, ~1180–1270 CE, ~1340–1410 CE, ~1450–1500 CE, and ~1540–1600 CE) shows significant sub-decadal power (2 to 12 years) in the wavelet analysis. The interannual frequencies resolved in the wavelet analysis are significant only during solar maxima (Fig. 4). This signifies that high solar irradiance coupled with ENSO feedbacks on the monsoon drives upwelling and diatom production in southern Lake Tanganyika, regardless of temperature effects on water column stratification. Least squares spectral analysis of Si/Ti confirms that ENSO band frequencies are statistically significant at 800–1000, 1000–1200, and 1400–1600 CE (fig. S4). El Niño tends to suppress the Indian Ocean monsoon over southeastern Africa, whereas La Niña enhances rainfall and wind speeds (*36*). Furthermore, NCAR (National Center for Atmospheric Research) ERA5 reanalysis data (1979–2019) show a significant negative correlation between upper-level winds and the Nino3.4 index near the LT17-2A site (fig. S5), indicating a probable link between monsoon wind intensity and La Niña. Rainfall proxy data from the central and western Pacific Ocean demonstrate that La Niña–like conditions dominated before ~900 CE and during the

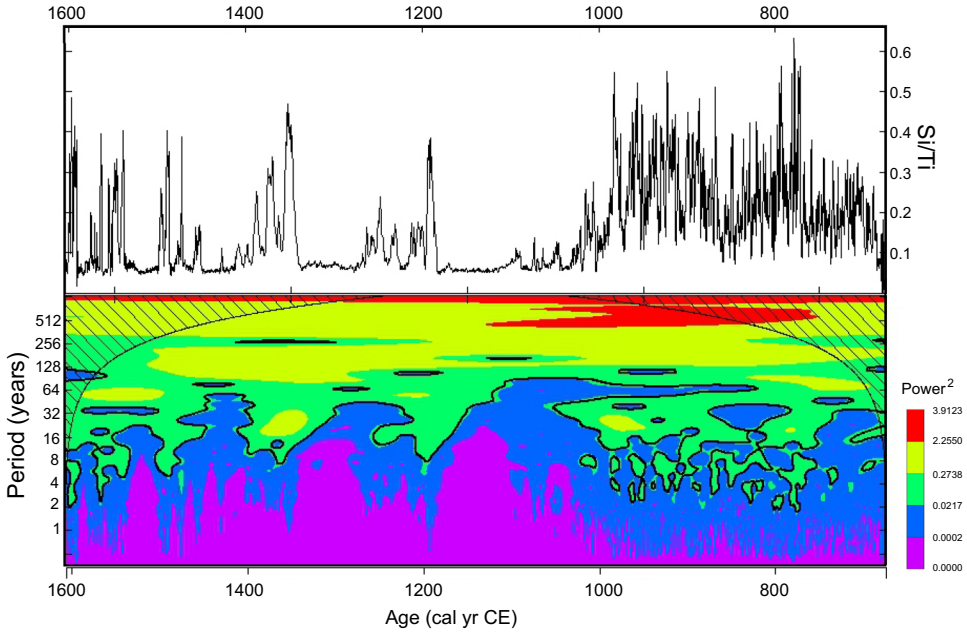

Fig. 4. Wavelet analysis of Si/Ti from core LT17-2A. The Fourier period is presented in years, and the thick black contour delineates >95% confidence interval. The cone of influence is indicated by the hatched area. The ~256- and 512-year bands are interpreted to reflect the influence of solar irradiance cycles, whereas the interannual frequencies most likely reflect ENSO.

Little Ice Age (Fig. 3) (*37*). Therefore, we conclude that convergence of a strong monsoon enhanced by high solar irradiance, La Niña, and cool surface waters results in strong upwelling and seasonal phytoplankton succession in southern Lake Tanganyika. In contrast, higher surface water temperatures and a monsoon weakened by low solar irradiance and El Niño, the conditions that occurred during the MCA, result in weak or absent upwelling, diminished seiche activity, and infrequent cyanobacteria blooms.

DISCUSSION

Dagaa populations respond rapidly to changes in ambient primary production (*5*). Our research indicates that future management of Lake Tanganyika, and analogous inland tropical fisheries, will benefit from strategies designed to cope with cyclic high-frequency changes in algal production. Conservation of Lake Tanganyika's *dagaa* is pivotal to the food security of rapidly growing and largely impoverished segments of four African nations (Tanzania, Democratic Republic of the Congo, Burundi, and Zambia). Reliable census data for this region are unavailable, but inland fishers in Africa are presently believed to exceed 2.7 million (*38*). Before our study, the climatic controls on energy flow within the pelagic food web were subject to considerable speculation. The changing influence of other external controls on the food web, most prominently human impacts (e.g., transitions toward agriculture, overfishing, and pollution), is beyond the scope of this study, as are internal drivers like evolution, population dynamics, self-organization of trophic levels, or feedbacks among species. Our study shows, however, that bottom-up trophic effects at Lake Tanganyika are perhaps dictated by atmospheric linkages to solar cycles and La Niña–like conditions, with surface water temperatures serving as a tipping point. Concerns surrounding the enhanced variability of the ENSO system under different scenarios of future warming are now well documented, and the socioeconomic threat to sub-Saharan Africa is the most severe of any region on Earth (*39*). The results of this study show that additional concern for the productivity of tropical inland fisheries is warranted.

MATERIALS AND METHODS

Core location

The most sensitive region of Lake Tanganyika for using sediments to reconstruct the lake-wide history of primary upwelling is the southern basin (Fig. 1A). Evidence for this is available from limnological sampling and remote sensing datasets, which have shown that wind-driven upwelling in southern Lake Tanganyika during the austral winter alters the lake-wide distribution of nutrients and results in a strong north-south phytoplankton gradient (*15*, *17*, *40*–*41*). In the northern basin, patchy nutrient delivery associated with seiches and secondary upwelling results in blooms of larger phytoplankton with complex and variable communities that shift among chlorophytes, filamentous cyanophytes, and diatoms (*15*). In contrast, upwelling in the southern basin produces more uniform algal communities dominated by *Nitzschia* diatoms that live in association with diazotrophic cyanobacteria. These southern basin algal communities and their dynamics therefore held the strongest potential to capture the signal of primary upwelling with well-understood geochemical and paleoecological tools. We located the coring station at 7.89610°S latitude and 30.76790° longitude, and the water depth was ~420 m in the southern basin to capture this signal. The site is located below the oxycline, resulting in excellent preservation of fine-scale sedimentary structures and organic matrices.

Geochemistry

Sub-annual resolution chemostratigraphic datasets (Si/Ti, Fe/Mn, and Ti) were produced using scanning x-ray fluorescence (XRF) at the University of Minnesota Duluth (Supplementary Materials).

Measurements were made every 0.02 cm downcore, resulting in an ultrahigh spatial density (n = 5401) dataset. Si/Ti is a well-established indicator of diatom abundance in African lake sediments (*42*), and our petrographic estimates of diatom valves per gram agree well with Si/Ti (fig. S1). Sponges, chrysophytes, and phytoliths can also contribute to the Si/Ti, but our observations demonstrated that Si/Ti overwhelmingly reflects diatom opal and that contributions from other siliceous microfossils are negligible. Fe/Mn is a sensitive indicator of lake floor oxygen levels and redox conditions in many large lakes (*22*). Previous sediment studies elsewhere in Lake Tanganyika have successfully fingerprinted wind-driven water column mixing and redox processes using XRF-derived Mn counts (*23*). Elemental Ti is a reliable indicator of detrital influx from the watershed to the lake, due to its exclusive association with minerals in continental crust (titanite, sphene, and ilmenite) and conservative behavior in the hydrosphere (fig. S3) (*22*).

The $^{15}N/^{14}N$ of bulk untreated sediment samples (hereafter referred to as $\delta^{15}N$) was measured at the University of Kentucky using isotope ratio mass spectrometry (Supplementary Materials). We assumed that organic sources of nitrogen dominate within the sediments and that the $\delta^{15}N$ reflects this signal. The $\delta^{15}N$ analysis was conducted at annual resolution (n = 181), and the precision was better than ±0.15‰. The principal controls on $\delta^{15}N$ are aqueous dissolved inorganic nitrogen concentrations, rates of photosynthesis, the dissolved N species available for uptake within the water column, and N sources (*25*). In Quaternary sediments from African rift lakes, $\delta^{15}N$ is often interpreted from the perspective of limnological changes influencing one or more of these factors.

Annual–to–multi-decadal resolution phosphorous geochemistry was determined at the Indiana State University. Sample size requirements for the analysis varied, and therefore, the sampling pattern was irregular along the length of the core (n = 52). A sequential extraction technique was used to measure total extractable P, and samples were analyzed using the molybdate blue technique with an ultraviolet-visible scanning spectrophotometer (*43*). Sequential extractions were used to isolate P associated with oxides and oxyhydroxides, mineral, and organic phases (fig. S2). Parsing out these phases is helpful for distinguishing among internal and external controls on the nutrient cycle. Detrital mineral-associated P burial is most often related to weathering and runoff (wetter climate), whereas organic P burial is associated with greater algal productivity.

Diatom paleoecology

Annual resolution diatom paleoecology was completed at the Indiana State University and the University of Arizona using standard techniques in optical and scanning electron microscopy. Each sample (n = 184) was examined under ×1000 magnification, and at least 300 valves were counted per slide (Supplementary Materials).

Statistical analysis

Power spectra of the chemostratigraphic data were analyzed using a continuous Morlet wavelet in the dplR package in R (*44*). This analysis was conducted to evaluate the frequency content throughout the Si/Ti time series, assuming nonstationarity of the important periods of variability. The Si/Ti data were interpolated to a uniform time step of 0.25 years before running the analysis. To verify significance of the high-resolution frequencies identified in the wavelet analysis, a Lomb-Scargle periodogram (fig. S4) was also applied to the Si/Ti dataset (Supplementary Materials). To evaluate the regional winds around Lake Tanganyika and their links to modern ENSO, we performed a spatial analysis using the ERA5 reanalysis dataset of the meridional wind component (v-wind) from 1979 to 2019 (fig. S5). A time series was calculated to represent the dry season when winds are strongest [June-July-August (JJA)], and this time series was trimmed spatially to capture only eastern Africa (40°S to 35°N; 20° to 55°E). The NINO3.4 sea surface temperature index time series was acquired over the same time interval and averaged over the same JJA season (*45*). The NINO3.4 time series was then correlated with the JJA meridional wind over East Africa gridcell by gridcell (Supplementary Materials).

SUPPLEMENTARY MATERIALS

Supplementary material for this article is available at http://advances.sciencemag.org/cgi/content/full/6/41/eabb2191/DC1

REFERENCES AND NOTES

1. R. L. Welcomme, I. G. Cowx, D. Coates, C. Béné, S. Funge-Smith, A. Halls, K. Lorenzen, Inland capture fisheries. *Philos. Trans. R. Soc. Lond. B Biol. Sci.* **365**, 2881–2896 (2010).
2. A. J. Lynch, S. J. Cooke, A. M. Deines, S. D. Bower, D. B. Bunnell, I. G. Cowx, V. M. Nguyen, J. Nohner, K. Phouthavong, B. Riley, M. W. Rogers, W. W. Taylor, W. Woelmer, S.-J. Youn, T. Douglas Beard Jr., The social, economic, and environmental importance of inland fish and fisheries. *Environ. Rev.* **24**, 115–121 (2016).
3. J. R. Porter, L. Xie, A. J. Challinor, K. Cochrane, S. M. Howden, M. M. Iqbal, D. Lobell, M. I. Travasso, Chapter 7: Food security and food production systems, in *Climate Change 2014: Impacts, Adaptation, and Vulnerability. Part A: Global and Sectoral Aspects. Contribution of Working Group II to the Fifth Assessment Report of the Intergovernmental Panel on Climate Change (IPCC 2014)* (Final Draft, IPCC AR5 WGII, Cambridge Univ. Press, 2014).
4. J. Kolding, P. van Zwieten, F. Marttin, S. Funge-Smith, F. Poulain, "Freshwater small pelagic fish and fisheries in the major African lakes and reservoirs in relation to food security and nutrition" (FAO Fisheries and Aquaculture Technical Paper 642, 2019); www.fao.org/3/ca0843en/ca0843en.pdf.
5. G. W. Coulter, *Lake Tanganyika and Its Life* (Oxford Univ. Press, 1991).
6. Y. Vadeboncoeur, P. B. McIntyre, M. J. Vander Zanden, Borders of biodiversity: Life at the edge of the world's large lakes. *Bioscience* **61**, 526–537 (2011).
7. U. M. Scharler, F. D. Hulot, D. J. Baird, W. F. Cross, J. M. Culp, C. A. Layman, D. Raffaelli, M. Vos, K. O. Winemueller, Central issues for aquatic food webs: From chemical cues to whole system responses, in *Dynamic Food Webs: Multispecies Assemblages, Ecosystem Development and Environmental Change,* P. C. de Ruiter, V. Wolters, J. C. Moore, Eds. (Elsevier, 2005).
8. C. M. O'Reilly, S. R. Alin, P.-D. Plisnier, A. S. Cohen, B. A. McKee, Climate change decreases aquatic ecosystem productivity of Lake Tanganyika, Africa. *Nature* **424**, 766–768 (2003).
9. P. Verburg, R. E. Hecky, H. Kling, Ecological consequences of a century of warming in Lake Tanganyika. *Science* **301**, 505–507 (2003).
10. A. S. Cohen, E. L. Gergurich, B. M. Kraemer, M. M. McGlue, P. B. McIntyre, J. M. Russell, J. D. Simmons, P. W. Swarzenski, Climate warming reduces fish production and benthic habitat in Lake Tanganyika, one of the most biodiverse freshwater ecosystems. *Proc. Natl. Acad. Sci. U.S.A.* **113**, 9563–9568 (2016).
11. J. E. Tierney, M. T. Mayes, N. Meyer, C. Johnson, P. W. Swarzenski, A. S. Cohen, J. M. Russell, Late-twentieth-century warming in Lake Tanganyika unprecedented since AD 500. *Nat. Geosci.* **3**, 422–425 (2010).
12. P. D. Plisnier, D. Chitamwebwa, L. Mwape, K. Tshibangu, V. Langenberg, E. Coenen, Limnological annual cycle inferred from physical-chemical fluctuations at three stations of Lake Tanganyika, in *From Limnology to Fisheries: Lake Tanganyika and Other Large Lakes* (Springer, 1999), pp. 45–58.
13. P. D. Plisnier, E. J. Coenen, Pulsed and dampened annual limnological fluctuations in Lake Tanganyika, in *The Great Lakes of the World (GLOW): Food-web, Health and Integrity*, M. Munawar, R. E. Hecky, Eds. (Ecovision World Monograph Series, 2001).
14. H. Kurki, I. Vuorinen, E. Bosma, D. Bwebwa, Spatial and temporal changes in copepod zooplankton communities of Lake Tanganyika, in *From Limnology to Fisheries: Lake Tanganyika and Other Large Lakes* (Springer, 1999), pp. 105–114.
15. R. E. Hecky, H. J. Kling, The phytoplankton and protozooplankton of the euphotic zone of Lake Tanganyika: Species composition, biomass, chlorophyll content, and spatio-temporal distribution. *Limnol. Oceanogr.* **26**, 548–564 (1981).
16. A. De Wever, K. Muylaert, D. Langlet, L. Alleman, J.-P. Descy, L. André, C. Cocquyt, W. Vyverman, Differential responses of phytoplankton to additions of nitrogen, phosphorus and iron in lake Tanganyika. *Freshw. Biol.* **53**, 264–277 (2008).

17. J.-P. Descy, M.-A. Hardy, S. Stenuité, S. Pirlot, B. Leporcq, I. Kimirei, B. Sekadende, S. R. Mwaitega, D. Sinyenza, Phytoplankton pigments and community composition in Lake Tanganyika. *Freshw. Biol.* **50**, 668–684 (2005).
18. S. Stenuite, A.-L. Tarbe, H. Sarmento, F. Unrein, S. Pirlot, D. Sinyinza, S. Thill, M. Lecomte, B. Leporcq, J. M. Gasol, J.-P. Descy, Photosynthetic picoplankton in Lake Tanganyika: Biomass distribution patterns with depth, season and basin. *J. Plankton Res.* **31**, 1531–1544 (2009).
19. A. S. Cohen, K. E. Lezzar, J. Cole, D. Dettman, G. S. Ellis, M. E. Gonneea, P.-D. Plisnier, V. Langenberg, M. Blaauw, D. Zilifi, Late Holocene linkages between decade–century scale climate variability and productivity at Lake Tanganyika, Africa. *J. Paleolimnol.* **36**, 189–209 (2006).
20. M. Blaauw, J. A. Christen, Flexible paleoclimate age-depth models using an autoregressive gamma process. *Bayesian Anal.* **6**, 457–474 (2011).
21. M. M. McGlue, K. E. Lezzar, A. S. Cohen, J. M. Russell, J.-J. Tiercelin, A. A. Felton, E. Mbede, H. H. Nkotagu, Seismic records of late Pleistocene aridity in Lake Tanganyika, tropical East Africa. *J. Paleolimnol.* **40**, 635–653 (2008).
22. S. J. Davies, H. F. Lamb, S. J. Roberts, Micro-XRF core scanning in palaeolimnology: Recent developments, in *Micro-XRF Studies of Sediment Cores* (Springer, 2015) pp. 189–226.
23. J. E. Tierney, J. M. Russell, Abrupt climate change in southeast tropical Africa influenced by Indian monsoon variability and ITCZ migration. *Geophys. Res. Lett.* **34**, L15709 (2007).
24. P. Kilham, S. S. Kilham, R. E. Hecky, Hypothesized resource relationships among African planktonic diatoms. *Limnol. Oceanogr.* **31**, 1169–1181 (1986).
25. M. R. Talbot, Nitrogen isotopes in palaeolimnology, in *Tracking Environmental Change Using Lake Sediments*, W. M. Last, J. P. Smol, Eds. (Springer, 2002), vol. 2, pp. 401–439.
26. M. R. Chapman, N. J. Shackleton, Evidence of 550-year and 1000-year cyclicities in North Atlantic circulation patterns during the Holocene. *Holocene* **10**, 287–291 (2000).
27. G. Bond, B. Kromer, J. Beer, R. Muscheler, M. N. Evans, W. Showers, S. Hoffmann, R. Lotti-Bond, I. Hajdas, G. Bonani, Persistent solar influence on North Atlantic climate during the Holocene. *Science* **294**, 2130–2136 (2001).
28. J. C. Stager, A. Ruzmaikin, D. Conway, P. Verburg, P. J. Mason, Sunspots, El Niño, and the levels of Lake Victoria, East Africa. *J. Geophys. Res. Atmos.* **112** (D15), D15106 (2007).
29. G. A. Meehl, J. M. Arblaster, G. Branstator, H. van Loon, A coupled air–sea response mechanism to solar forcing in the Pacific region. *J. Climate* **21**, 2883–2897 (2008).
30. H. van Loon, G. A. Meehl, J. M. Arblaster, A decadal solar effect in the tropics in July – August. *J. Atmos. Sol. Terr. Phys.* **66**, 1767–1778 (2004).
31. F. Steinhilber, J. A. Abreu, J. Beer, I. Brunner, M. Christl, H. Fischer, U. Heikkilä, P. W. Kubik, M. Mann, K. G. McCracken, H. Miller, H. Miyahara, H. Oerter, F. Wilhelms, 9,400 years of cosmic radiation and solar activity from ice cores and tree rings. *Proc. Natl. Acad. Sci. U.S.A.* **109**, 5967–5971 (2012).
32. M. E. Mann, Z. Zhang, S. Rutherford, R. S. Bradley, M. K. Hughes, D. Shindell, C. Ammann, G. Faluvegi, F. Ni, Global signatures and dynamical origins of the Little Ice Age and Medieval Climate Anomaly. *Science* **326**, 1256–1260 (2009).
33. S. R. Alin, A. S. Cohen, Lake-level history of Lake Tanganyika, East Africa, for the past 2500 years based on ostracode-inferred water-depth reconstruction. *Palaeogeogr. Palaeoclimatol. Palaeoecol.* **199**, 31–49 (2003).
34. S. E. Nicholson, The nature of rainfall variability over Africa on time scales of decades to millenia. *Glob. Planet. Change* **26**, 137–158 (2000).
35. P. D. Plisnier, S. Serneels, E. F. Lambin, Impact of ENSO on East African ecosystems: A multivariate analysis based on climate and remote sensing data. *Glob. Ecol. Biogeogr.* **9**, 481–497 (2000).
36. P. X. Wang, B. Wang, H. Cheng, J. Fasullo, Z. Guo, T. Kiefer, Z. Liu, The global monsoon across time scales: Mechanisms and outstanding issues. *Earth Sci. Rev.* **174**, 84–121 (2017).
37. H. Yan, L. Sun, Y. Wang, W. Huang, S. Qiu, C. Yang, A record of the Southern Oscillation Index for the past 2,000 years from precipitation proxies. *Nat. Geosci.* **4**, 611–614 (2011).
38. S. Funge-Smith, A. Bennett, A fresh look at inland fisheries and their role in food security and livelihoods. *Fish Fish.* **20**, 1176–1195 (2019).
39. I. Niang, O. C. Ruppel, M. A. Abdrabo, A. Essel, C. Lennard, J. Padgham, P. Urquhart, Africa Climate Change 2014: Impacts, adaptation, and vulnerability, in *Contribution of Working Group II to the Fifth Assessment Report of the Intergovernmental Panel on Climate Change* (Cambridge Univ. Press, 2014), pp. 1199–1265.
40. K. Vuorio, M. Nuottajärvi, K. Salonen, J. Sarvala, Spatial distribution of phytoplankton and picocyanobacteria in Lake Tanganyika in March and April 1998. *Aquat. Ecosyst. Health* **6**, 263–278 (2003).
41. A. De Wever, K. Muylaert, C. Cocquyt, J. Van Wichelen, P.-D. Plisnier, W. Vyverman, Seasonal and spatial variability in the abundance of auto-and heterotrophic plankton in Lake Tanganyika. *Fund. Appl. Limnol.* **170**, 49–63 (2007).
42. E. T. Brown, T. C. Johnson, C. A. Scholz, A. S. Cohen, J. W. King, Abrupt change in tropical African climate linked to the bipolar seesaw over the past 55,000 years. *Geophys. Res. Lett.* **34**, L20702 (2007).
43. L. D. Anderson, M. L. Delaney, Sequential extraction and analysis of phosphorus in marine sediments: Streamlining of the SEDEX procedure. *Limnol. Oceanogr.* **45**, 509–515 (2000).
44. A. Bunn, M. Korpela, F. Biondi, F. Campelo, P. Mérian, F. Qeadan, C. Zang, dplR: Dendrochronology Program Library in R. R package version 1.7.0 (2019); https://CRAN.R-project.org/package=dplR.
45. N. A. Rayner, D. E. Parker, E. B. Horton, C. K. Folland, L. V. Alexander, D. P. Rowell, E. C. Kent, A. Kaplan, Global analyses of sea surface temperature, sea ice, and night marine air temperature since the late nineteenth century. *J. Geophys. Res.* **108** (D14), 4407 (2003).
46. J. C. Stager, C. Cocquyt, R. Bonnefille, C. Weyhenmeyer, N. Bowerman, A late Holocene paleoclimatic history of Lake Tanganyika, East Africa. *Quat. Res.* **72**, 47–56 (2009).
47. A. S. Cohen, M. R. Talbot, S. M. Awramik, D. L. Dettman, P. Abell, Lake level and paleoenvironmental history of Lake Tanganyika, Africa, as inferred from late Holocene and modern stromatolites. *Geol. Soc. Am. Bull.* **109**, 444–460 (1997).
48. A. A. Felton, J. M. Russell, A. S. Cohen, M. E. Baker, J. T. Chesley, K. E. Lezzar, M. M. McGlue, J. S. Pigati, J. Quade, J. C. Stager, J. J. Tiercelin, Paleolimnological evidence for the onset and termination of glacial aridity from Lake Tanganyika, Tropical East Africa. *Palaeogeogr. Palaeoclimatol. Palaeoecol.* **252**, 405–423 (2007).
49. K. Fontijn, G. G. J. Ernst, M. A. Elburg, D. Williamson, E. Abdallah, S. Kwelwa, E. Mbede, P. Jacobs, Holocene explosive eruptions in the Rungwe Volcanic Province, Tanzania. *J. Volcanol. Geotherm. Res.* **196**, 91–110 (2010).
50. C. M. O'Reilly, D. L. Dettman, A. S. Cohen, Paleolimnological investigations of anthropogenic environmental change in Lake Tanganyika: VI. Geochemical indicators. *J. Paleolimnol.* **34**, 85–91 (2005).
51. R. W. Battarbee, V. J. Jones, R. J. Flower, N. G. Cameron, H. Bennion, L. Carvalho, S. Juggins, Diatoms, in *Tracking Environmental Change Using Lake Sediments* (Springer, 2002), pp. 155–202.
52. C. Cocquyt, *Diatoms from the Northern Basin of Lake Tanganyika* (Bibliotheca Diatomologica 39, 1998).
53. F. Gasse, *East African Diatoms: Taxonomy, Ecological Distribution* (Bibliotheca Diatomologica 11, 1986).
54. Ø. Hammer, D. A. T. Harper, P. D. Ryan, PAST: Paleontological statistics software package for education and data analysis. *Palaeontol. Electron.* **4**, 9 (2001).
55. W. H. Press, S. A. Teukolsky, W. T. Vetterling, B. P. Flannery, *Numerical Recipes in C* (Cambridge Univ. Press, 1992).
56. M. Sigl, M. Winstrup, J. R. McConnell, K. C. Welten, G. Plunkett, F. Ludlow, U. Büntgen, M. Caffee, N. Chellman, D. Dahl-Jensen, H. Fischer, S. Kipfstuhl, C. Kostick, O. J. Maselli, F. Mekhaldi, R. Mulvaney, R. Muscheler, D. R. Pasteris, J. R. Pilcher, M. Salzer, S. Schüpbach, J. P. Steffensen, B. M. Vinther, T. E. Woodruff, Timing and climate forcing of volcanic eruptions for the past 2,500 years. *Nature* **523**, 543 (2015).

Acknowledgments: We thank the Tanzania Commission for Science and Technology (COSTECH) for authorizing the research (2016-300-ER-2011-87); the Tanzania Fisheries Research Institute Kigoma Station and the Nature Conservancy for logistics assistance; J. Lucas, E. Ryan, A. Mbonde, M. Mupape, and the crew of the *M/V Maman Benita* for field assistance; the LacCore staff and R. Brown for core curation, processing, and XRF assistance; H. Bierly and E. Smith for assistance with diatom sample preparation; R. Gaines for assistance with P extraction; and J. Russell, S. Fritz, P. McIntyre, D. Carden, G. Ellis, C. Apse, and two anonymous reviewers for comments and discussion on early drafts. **Funding:** This research was supported by the University of Kentucky-Pioneer Endowment, SEG-Geoscientists Without Borders (201401005), and the U.S. NSF (EAR-1424907). **Author contributions:** M.M.M. designed the study. S.J.I. completed the statistical analysis. J.R.S. and T.M.K. completed the diatom analysis. J.C.L. produced the P dataset. M.M.M. and M.A.B. developed the nitrogen data. M.M.M., M.J.S., and I.A.K. coordinated the research in the field. M.M.M., S.J.I., and J.R.S. prepared the manuscript. All the authors analyzed the data and reviewed the manuscript. **Competing interests:** The authors declare that they have no competing interests. **Data and materials availability:** All data needed to evaluate the conclusions in the paper are present in the paper and/or the Supplementary Materials. Additional data related to this paper may be requested from the authors.

Submitted 8 February 2020
Accepted 20 August 2020
Published 9 October 2020
10.1126/sciadv.abb2191

Citation: M. M. McGlue, S. J. Ivory, J. R. Stone, A. S. Cohen, T. M. Kamulali, J. C. Latimer, M. A. Brannon, I. A. Kimirei, M. J. Soreghan, Solar irradiance and ENSO affect food security in Lake Tanganyika, a major African inland fishery. *Sci. Adv.* **6**, eabb2191 (2020).